



Applications of the Proper Orthogonal Decomposition Method

Internship report

Katrin GRAU
Mentoring: Laurent GICQUEL

September 2007

WN/CFD/07/97

I would like to thank the whole CFD team at CERFACS, in particular

- L. Gicquel, my supervisor, for his excellent mentoring and support,
- A. Roux, who explained his codes to me and helped me with all the occurring problems,
- M. Leyko, for providing me the snapshots for the applications and discussing the results,
- T. Poinso, for the opportunity to do an internship in the CFD team at CERFACS.

Contents

1	Introduction	2
2	Proper Orthogonal Decomposition Method	2
3	Application: “Perfect” Square	4
3.1	Theory	4
3.2	AVBP	6
3.3	Proper Orthogonal Decomposition	6
3.3.1	Pressure fluctuation	7
3.3.2	Velocity fluctuation	8
3.3.3	Pressure and velocity fluctuation	10
3.4	Conclusions	13
4	Application: Square	13
4.1	AVBP	13
4.2	Proper Orthogonal Decomposition	14
4.3	Conclusions	18
5	Application: Square, 3 initial modes	19
5.1	AVBP	19
5.2	Proper Orthogonal Decomposition	20
5.3	Conclusions	21
6	Application: L-Shape	23
6.1	AVBP	23
6.2	Proper Orthogonal Decomposition	25
6.3	Conclusions	26
7	Conclusions	26
	Annex	29

1 Introduction

With the increase of the capacity of computers used for numerical simulations the amount of produced data has increased as well. These large amounts of data have to be analyzed to gain a better understanding of the simulated processes.

The Proper Orthogonal Decomposition (POD) is a post-processing technique. It takes a given set of data and extracts basis functions, that contain as much “energy” as possible. The meaning of “energy” depends on which kind of POD is used.

One problem that occurs is the choice of variables that should be taken into account while using POD. If the numerical simulation is made for incompressible flows, only the velocity is a variable of interest. In a compressible flow, the pressure becomes important as well and should be included when performing POD.

The object of this internship was to test the existing POD tool at CERFACS using different academic applications to investigate the effect of the chosen inner product.

2 Proper Orthogonal Decomposition Method

An overview over the POD method can be found for example in [4], but a short summary of the parts of POD relevant for the following applications is given here (see [1], [2], [3], [4], [5], [6], [10]).

Let $q_k(x), k = 1 \dots N_t$, be a set of observations (called “snapshots”) at points $x \in \Omega$, that could be obtained by a numerical simulation or experimental measurements. The goal of POD is to find functions ϕ such that

$$\frac{\langle |q, \phi|^2 \rangle}{\|\phi\|^2} \tag{1}$$

is maximized. $\langle . \rangle$ is some kind of average, $(., .)$ is an inner product and $\|\cdot\|$ the induced norm. The functions ϕ span a subspace of the original space of the snapshots $q_k(x)$ such that the error of the orthogonal projection is minimized. Solving the optimization problem leads to an eigenvalue problem, where the functions ϕ are the eigenfunctions.

Two different types of POD exist, the classical (see [7]) and the snapshot POD (see [13]). The latter is used here. The idea of the snapshot POD is not to solve the eigenvalue problem to obtain the functions ϕ (where the dimension would depend on the number of points), but to write ϕ depending on the given snapshots:

$$\phi(x) = \sum_{k=1}^{N_t} a_k q_k(x), \tag{2}$$

which leads to the task of solving the eigenvalue problem

$$CA = \lambda A, \tag{3}$$

where

$$A = \begin{pmatrix} a_1 \\ a_2 \\ \vdots \\ a_{N_t} \end{pmatrix} \quad \text{and} \quad c_{ij} = \frac{1}{N_t} (q_i(x), q_j(x)) \quad (4)$$

C is called the correlation matrix (which is a $N_t \times N_t$ -matrix) and the inner product (\cdot, \cdot) has to be chosen suitably and will be discussed later.

The eigenvectors A^l found by solving Eq. (3) and sorted by the corresponding eigenvalue λ^l in descending order are scaled such that

$$\sum_{k=1}^{N_t} a_k^i a_k^j = N_t \lambda^i \delta_{ij}, \quad (5)$$

where δ_{ij} is the Kronecker delta. $\phi^l(x)$ is calculated as follows (to produce normalized functions):

$$\phi^l(x) = \frac{1}{N_t \lambda^l} \sum_{k=1}^{N_t} a_k^l q_k(x). \quad (6)$$

The “energy” corresponding to a function $\phi^l(x)$ is given by λ^l , but what exactly this “energy” is depends on the definition of the inner product used in Eq. (4). For different choices of the inner product see for example [11], [6] and [9].

The functions $\phi^l(x), l = 1, \dots, M$, will be called spatial eigenvectors or POD modes and A^l will be called temporal eigenvectors as the different snapshots $q_k(x)$ might be snapshots at different points in time $t_k, k = 1, \dots, N_t$, such that $q_k(x) = q(x, t_k)$. So the components a_k^l of the eigenvector A^l are the temporal coefficients $a^l(t_k)$ for the spatial eigenvectors ϕ^l :

$$q(x, t) \approx \sum_{l=1}^M a^l(t) \phi^l(x) \quad (7)$$

The choice of the inner product is an important part for the use of the POD method. Different inner products are available and which one should be used depends on the given snapshots. For incompressible flows the usual variable of interest is the velocity $q(x, t) = (u(x, t), v(x, t), w(x, t))$ in 3D. Then the inner product should be defined as follows:

$$(q_k(x), q_l(x)) = \int_{\Omega} (u_k(x)u_l(x) + v_k(x)v_l(x) + w_k(x)w_l(x)) dx, \quad (8)$$

where the indices k, l stand for different points in time t_k and t_l .

If the flow is compressible, not only the velocity should be taken into account but as well the pressure p . It is possible to use the same inner product as for incompressible flows (see Eq. (8)), but only the information of the velocity will be used in this case. In the context of compressible flow, acoustic fields are of interest and that information is entirely contained in the pressure variable if there is no mean flow. The inner product is thus defined as follows:

$$(q_k(x), q_l(x)) = \int_{\Omega} \frac{p_k(x)p_l(x)}{\bar{\rho}^2 \bar{c}^2} dx, \quad (9)$$

where $\bar{\rho}(x)$ and $\bar{c}(x)$ are the mean temporal density and speed of sound.

For complex acoustic fields velocity and pressure contain information about the acoustic field and both quantities have to be part of the inner product. Usually only fluctuating coherent structures are of interest¹, so that only the fluctuations are retained, $q(x, t) = (u', v', w', p')$ and the inner product reads:

$$(q_k(x), q_l(x)) = \int_{\Omega} (u'_k(x)u'_l(x) + v'_k(x)v'_l(x) + w'_k(x)w'_l(x) + \frac{p'_k(x)p'_l(x)}{\bar{\rho}^2\bar{c}^2})dx, \quad (10)$$

Another choice that has to be made is how many POD modes should be calculated (determine M , see Eq. (7)). If the corresponding eigenvalue λ^l is very small, ϕ^l contains not much energy. So to interpret the POD modes the corresponding eigenvalue has to be kept in mind.

3 Application: “Perfect” Square

The first application that is considered is given for a 2D square computational domain and will be purely acoustic. The intention is to get an analytical solution (of the wave equation) and test if the POD method is able to find the eigenmode/eigenmodes.

3.1 Theory

More about the theory of acoustics can be found in [8], Chapter 8, where a similar derivation is given. A QPF for AVSP on a 2D square with theoretical considerations is found in [12].

Assuming harmonic waves, spatial and temporal fluctuations of the pressure p' may be decoupled by writing:

$$p' = \text{Re} \left(\hat{p}e^{(-i\omega t)} \right). \quad (11)$$

In a homogeneous isentropic flow, linearizing the continuity and momentum equations leads to the Helmholtz equation:

$$\nabla^2 \hat{p} + k^2 \hat{p} = 0 \quad (12)$$

with the dispersion relation for a homogeneous medium

$$k^2 = \left(\frac{\omega}{c_0} \right)^2 \quad (13)$$

where c_0 is the mean sound speed.

Regarding the geometry (see Fig. 1) it is assumed that the solution for Eq. (12) is given in the following form:

$$\hat{p}(x, y) = X(x)Y(y). \quad (14)$$

¹Note that the first POD mode yields the mean value of the snapshots

Substituting this expression (14) in Eq. (12) leads to:

$$\frac{X''}{X} + \frac{Y''}{Y} + k^2 = 0. \quad (15)$$

Using $k^2 = k_x^2 + k_y^2$ Eq. (15) can be split as follows:

$$\begin{aligned} \frac{X''}{X} + k_x^2 &= 0 \\ \frac{Y''}{Y} + k_y^2 &= 0 \end{aligned} \quad (16)$$

The boundary conditions are:

$$\begin{aligned} \frac{dX}{dx}(0) &= 0, \\ \frac{dX}{dx}(L) &= 0, \\ \frac{dY}{dy}(0) &= 0, \\ \frac{dY}{dy}(L) &= 0 \end{aligned} \quad (17)$$

The solution of Eq. (16) with boundary conditions (Eq. (17)) is:

$$\begin{aligned} X(x) &= \cos(k_x x) \\ Y(y) &= \cos(k_y y), \end{aligned} \quad (18)$$

where the wave numbers k_x and k_y must satisfy:

$$\begin{aligned} \sin(k_x L) &= 0 \\ \sin(k_y L) &= 0, \end{aligned} \quad (19)$$

so

$$\begin{aligned} k_x &= \frac{n_x \pi}{L} \\ k_y &= \frac{n_y \pi}{L}, \end{aligned} \quad (20)$$

where n_x, n_y are positive integers. So the acoustic eigenmodes are

$$\hat{p} = P_{amp} \cdot \cos(n_x \cdot \pi \cdot \frac{x}{L}) \cos(n_y \cdot \pi \cdot \frac{y}{L}) \quad (21)$$

Solutions for p', u' and v' are

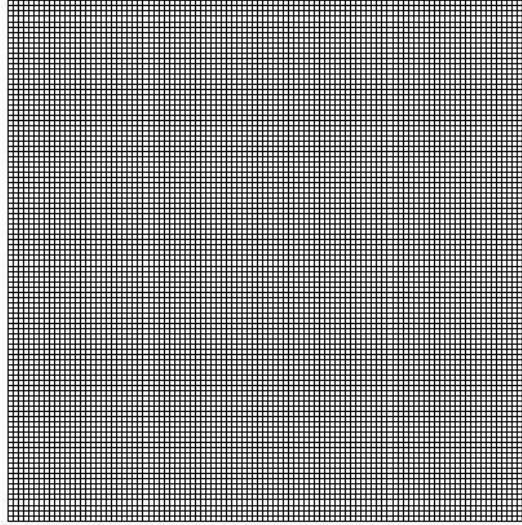


Figure 1: Grid used for AVBP solution, “perfect” square

$$p'(x, y, t) = P_{amp} \cdot \cos(n_x \cdot \pi \cdot \frac{x}{L}) \cos(n_y \cdot \pi \cdot \frac{y}{L}) \cos(-\omega t - \frac{\pi}{2}) \quad (22)$$

$$u'(x, y, t) = -\frac{P_{amp}\pi n_x}{\rho_0\omega L} \cdot \sin(n_x \cdot \pi \cdot \frac{x}{L}) \cos(n_y \cdot \pi \cdot \frac{y}{L}) \cos(-\omega t - \pi) \quad (23)$$

$$v'(x, y, t) = -\frac{P_{amp}\pi n_y}{\rho_0\omega L} \cdot \cos(n_x \cdot \pi \cdot \frac{x}{L}) \sin(n_y \cdot \pi \cdot \frac{y}{L}) \cos(-\omega t - \pi) \quad (24)$$

3.2 AVBP

The AVBP snapshots have been provided by M. Leyko, but a short description is given here. The grid used for the AVBP solution is shown in Fig. 1, which uses 100 nodes in each direction.

Although the POD code uses snapshots in the “format” of an AVBP solution, this first application is not the result of a real AVBP run. The results are generated based on Eq. (22)-(24), using $n_x = n_y = 1$ and they are only in the format of an AVBP solution.

3.3 Proper Orthogonal Decomposition

To obtain a POD from the given snapshots of the AVBP solution the key variable has to be chosen. It specifies the inner product that is used for the calculation of the correlation matrix. To get a better understanding of the effect of the inner product used in the POD analysis, three different inner products are applied for the same AVBP snapshots:

- inner product for pressure fluctuation
- inner product for velocity fluctuation
- inner product for pressure and velocity fluctuation

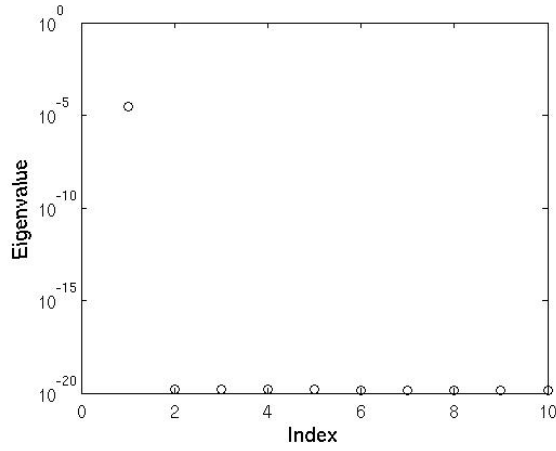


Figure 2: Eigenvalues, “perfect” square, pressure fluctuation

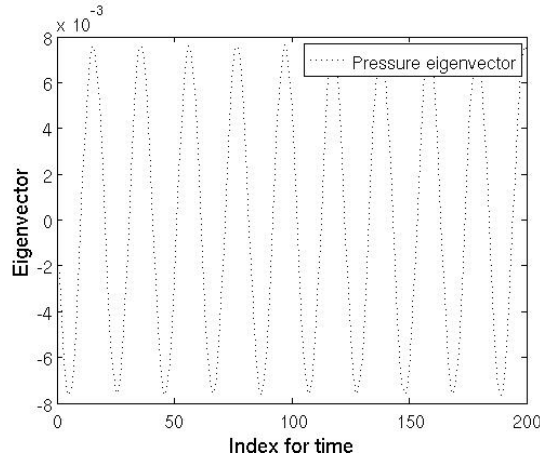


Figure 3: First temporal eigenvector evolution, “perfect” square, pressure fluctuation

3.3.1 Pressure fluctuation

The inner product used for the calculation of the correlation matrix is numerically defined as follows (see Eq. (4) and (9)):

$$c_{ij} = \frac{1}{N_t} \sum_{n=1}^{N_{pts}} \frac{p_i^n p_j^n}{\bar{\rho}^2 \bar{c}^2} \cdot \text{voln}(n), \quad (25)$$

where p_i^n is the pressure fluctuation at the n -th point and the i -th time step and $\text{voln}(n)$ is the nodal volume. The i -th time step is the i -th snapshot. The key variable is called “PressureFluc” and 200 snapshots are used to calculate 10 POD modes.

Figure 2 shows the first 10 eigenvalues. The importance of the temporal and spatial eigenvector is given by the eigenvalue. Only the first one has to be considered as the following eigenvalues are too small to be of interest. Thus only the first temporal eigenvector and the first POD mode have to be considered. Figure 3 shows the evolution of the first temporal eigenvector. Each component of the eigenvector belongs to one time step, so every index i stands for the time t_i .

The first POD mode (first spatial eigenvector) is shown in Fig. 4.

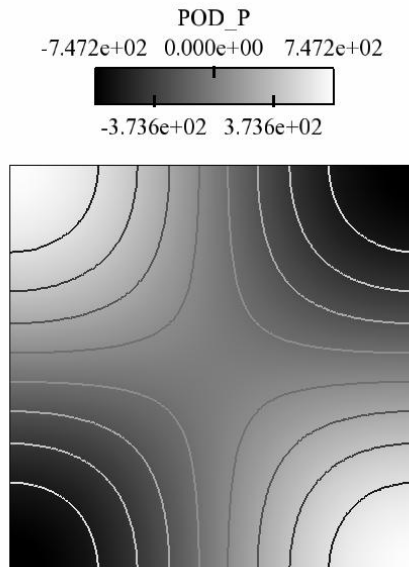


Figure 4: First POD mode, “perfect” square, pressure fluctuation

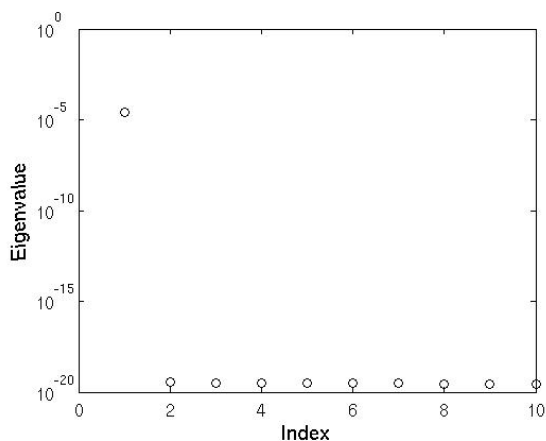


Figure 5: Eigenvalues, “perfect” square, velocity fluctuation

3.3.2 Velocity fluctuation

The next inner product that is used to calculate the correlation matrix is the following (see Eq. (4) and (8)):

$$c_{ij} = \frac{1}{N_t} \sum_{n=1}^{N_{pts}} (u_i^n u_j^n + v_i^n v_j^n) \cdot \text{voln}(n), \quad (26)$$

where u_i^n is the velocity fluctuation in the first direction at the n -th point and the i -th time step, v_i^n the velocity fluctuation in the second direction at the n -th point and the i -th time step and $\text{voln}(n)$ is the nodal volume. The same snapshots are used as in section 3.3.1, 10 POD modes have been calculated and the key variable is “primevelocity”.

Figure 5 shows the first 10 eigenvalues, and again only the first one has to be considered (the others are too small).

As pressure and velocity are connected, the evolution of the temporal eigenvectors for pressure and the velocity fluctuations are connected as well. This can be seen in Fig. 6, where not only the temporal eigenvector of the POD for the velocity fluctuation is shown but also is the first temporal eigenvector of the POD for the pressure fluctuation (see Fig. 3 of section 3.3.1). The shift between pressure and velocity is $\frac{\pi}{2}$, as it should be due to Eq. (22)-(24).

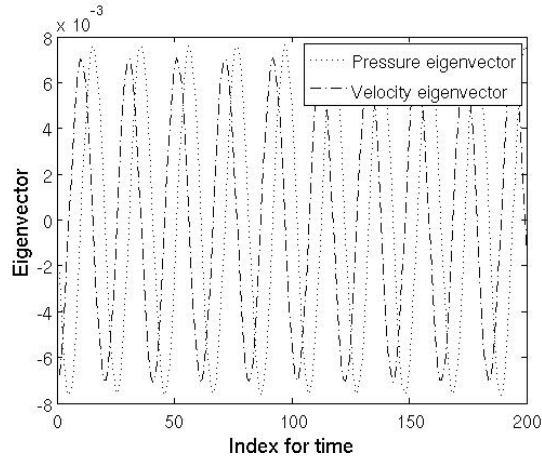


Figure 6: First temporal eigenvector evolution, “perfect” square, pressure and velocity fluctuation

Figure 7 shows the first POD mode, split into two modes as the velocity has two components:

- velocity u
- velocity v

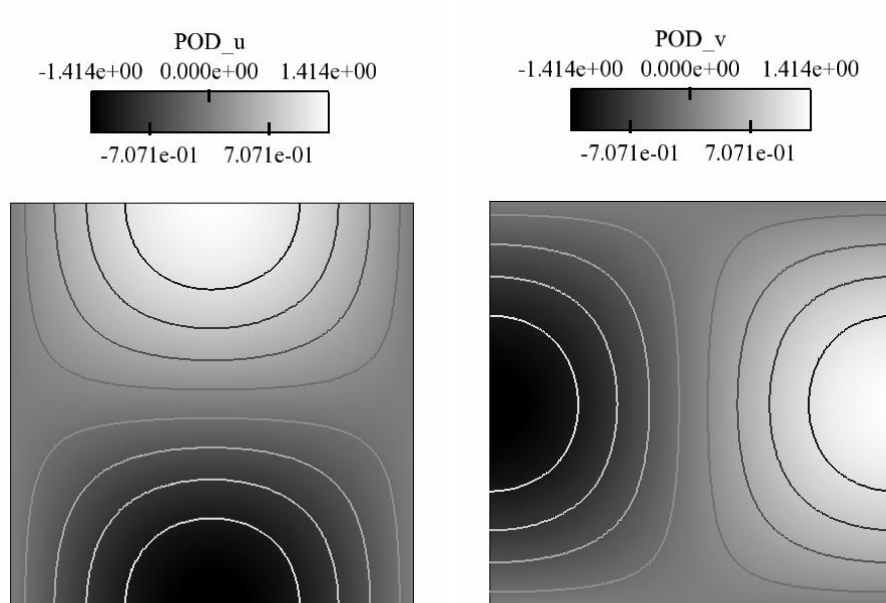


Figure 7: First POD mode, “perfect” square, velocity fluctuation

3.3.3 Pressure and velocity fluctuation

The key variable for the third calculation with the same snapshots is “acousEnFluc”, which means that the correlation matrix C is calculated with the following inner product (see Eq. (4) and (10)):

$$c_{ij} = \frac{1}{N_t} \sum_{n=1}^{N_{pts}} (u_i^n u_j^n + v_i^n v_j^n + \frac{p_i^n p_j^n}{\rho^2 c^2}) \cdot \text{voln}(n), \quad (27)$$

where u_i^n is the velocity component in the first direction at the n -th point and the i -th time step, v_i^n the velocity component in the second direction at the n -th point and the i -th time step, p_i^n the pressure at the n -th point and the i -th time step and $\text{voln}(n)$ is the nodal volume. Note that the mean value is again subtracted to consider only the fluctuations.

200 snapshots are used to calculate 10 POD modes. Although 10 modes have been calculated, only the first two have to be considered. Figure 8 shows the first 20 eigenvalues.

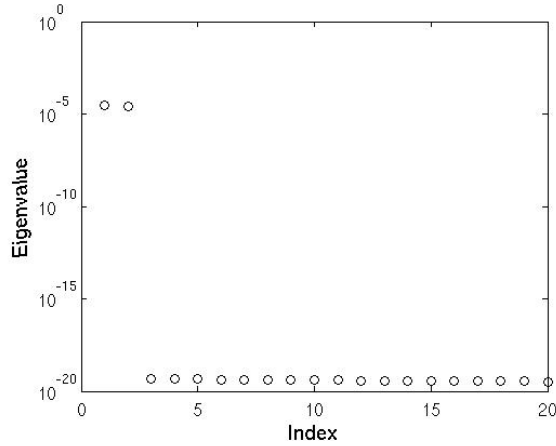


Figure 8: Eigenvalues, “perfect” square, acoustic energy fluctuation

The first two eigenvalues are clearly bigger than the rest. The two temporal eigenvectors of these two eigenvalues are linked, as shown in Fig. 9, one corresponding to the pressure evolution and the second to velocity.

Figure 10 shows the evolution of the first and second temporal eigenvector. They are shifted by $\frac{\pi}{2}$, as p' and u' are in Eq. (22) and Eq. (23) respectively. Figure 10 reminds very much of Fig. 6 in section 3.3.2, only with a phase-shift for the pressure.

As mentioned before 10 POD modes have been calculated, but only the first two are interesting. For the key variable “acousEnFluc” the solution for the spatial eigenvectors, the POD modes, are split in three parts:

- pressure p
- velocity u
- velocity v

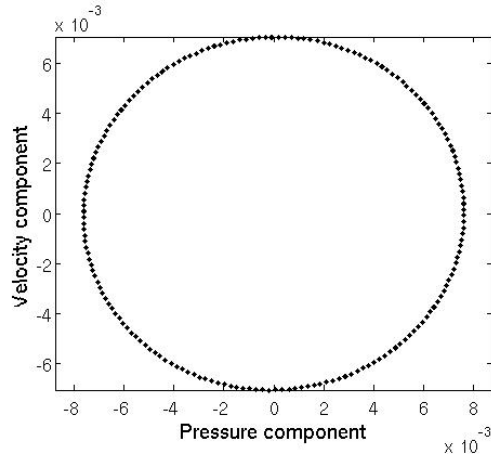


Figure 9: First and second temporal eigenvector, “perfect” square, acoustic energy fluctuation

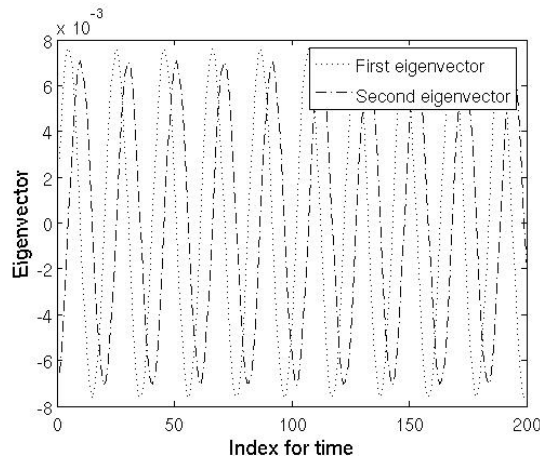


Figure 10: First and second temporal eigenvector evolution, “perfect” square, acoustic energy fluctuation

To get the “real” POD mode, these three parts have to be considered together. u and v are essentially the same, only with interchanged axis (see Eq. (23) and (24)). Figure 11 and 12 show the first and the second POD modes for u , v and p (v only for the first one). These two POD modes seem to be almost the same, which is not surprising: Even though one is linked to the pressure and the other one to the velocity due to their temporal eigenvectors, pressure and velocity are linked to each other. A closer look at the scaling shows that the POD mode for u is getting stronger from the first to the second mode (maximal value goes from $1.155e - 01$ to $1.409e + 00$), while the POD mode for p is getting weaker (maximal value goes from $7.447e + 02$ to $6.102e + 01$). For the velocity the parts where the maximum and the minimum is reached are switched. So if they are put together in the one real POD mode, it won't be twice the same mode.

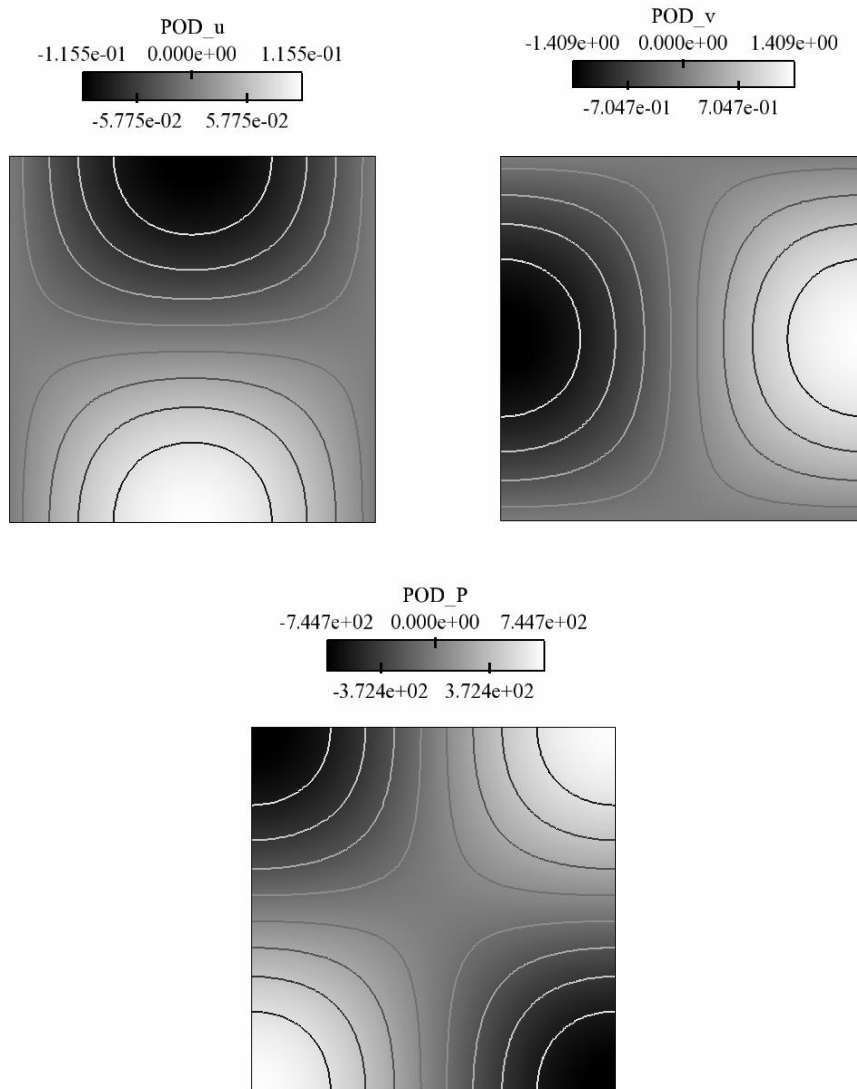


Figure 11: First POD mode, "perfect" square, acoustic energy fluctuation

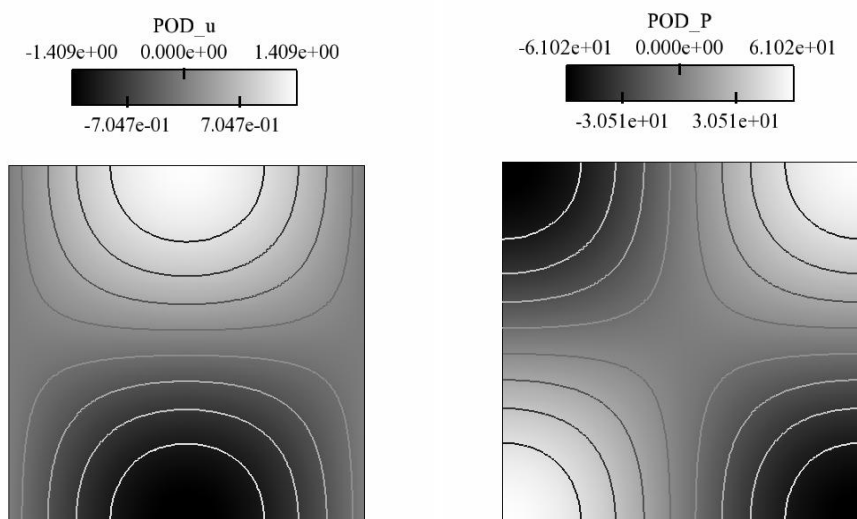


Figure 12: Second POD mode, "perfect" square, acoustic energy fluctuation

3.4 Conclusions

The first application is a theoretical example, where the POD analysis is used for a perfect solution to get to know how the results have to be interpreted.

The POD analysis is able to find the main (and only) mode in both pressure and velocity. The inner product based on the acoustic energy fluctuation leads to “double” modes due to the connection between velocity and pressure.

4 Application: Square

The second application is again given on the square in 2D (see Fig. 1), in fact the same square as in section 3, 100×100 nodes. This time a “real” AVBP solution is used for the POD analysis. The theory of this example is the same as in section 3 and can be found in section 3.1.

4.1 AVBP

The snapshots for this application have been provided by M. Leyko. A short description is given here.

The grid used for the AVBP solution is the same as in section 3 (see Fig. 1).

The initial solution is again the theoretical solution with $n_x = n_y = 1$ and was used in section 3.

run.dat file and asciibound file

The run.dat file used to generate the AVBP solution:

```
'../MESH/carre2'! Mesh file
'./carre.asciiBound' ! AsciiBound file
'dummy' ! AsciiBound_tpf file
'../SOLUTBOUND/carre2.solutBound'! Boundary solution file
'../INIT/init.h5'
'./SOLUTIONS/carre.sol'! output files
'./TIME01/'! temporal evolution directory

1.0d0      ! Reference length | scales coordinates X by X/reflen

1000000    ! Number of iterations

40         ! Number of elements per group (typically of order 100)
1         ! Preprocessor: skip (0), use (1) & write (2) & stop (3)

1         ! Interactive details of convergence (1) or not (0)
1         ! Prints convergence every x iterations
2         ! Stores solution in separate files (1) or not (0)
10.0d-2    ! final physical time
20.0d-5    ! storage time interval

0         ! Euler (0) or Navier-Stokes (1) calculation
```

```

0      ! Additional
0      ! Chemistry
0      ! LES
0      ! TPF
0      ! Artificial viscosity
1      ! Steady state (0) or unsteady (1) calculation

0 0 0 0 0    ! Scheme specification
3          ! Number of Runge-Kutta stages
0.333333d0 0.5d0 1.0d0    ! Runge-Kutta coefficients
0.7d0      ! CFL parameter for complete update
0.000d0    ! 4th order artificial viscosity coeff.
0.000d0    ! 2nd order artificial viscosity coeff.
0.1d0     ! Fourier parameter for viscous time-step

```

The ascibound file used is:

```

Grid processing by hip version 1.19 'Aardvark'.
4 boundary patches.

```

```

-----
Patch: 1
bottom: y=0
WALL_SLIP_ADIAB

```

```

-----
Patch: 2
right: x=1
WALL_SLIP_ADIAB

```

```

-----
Patch: 3
top: y=1
WALL_SLIP_ADIAB

```

```

-----
Patch: 4
left: x=0
WALL_SLIP_ADIAB

```

4.2 Proper Orthogonal Decomposition

The inner product “acousEnFluc” is used for the POD analysis as in section 3 (see Eq. (27)). Again 200 snapshots are used and 10 POD modes are calculated.

The avbp2pod.choices file used for the POD analysis is (see annex for further explanation):

```

'./POD_acousEnFluc_scaled/carre.pod'    !-! Output Solution
'../RUN/SOLUTIONS/carre.sol'           !-! Solution Pattern
0000001                                 !-! Initial Solution
0000200                                 !-! Final Solution
0000001                                 !-! Step

```

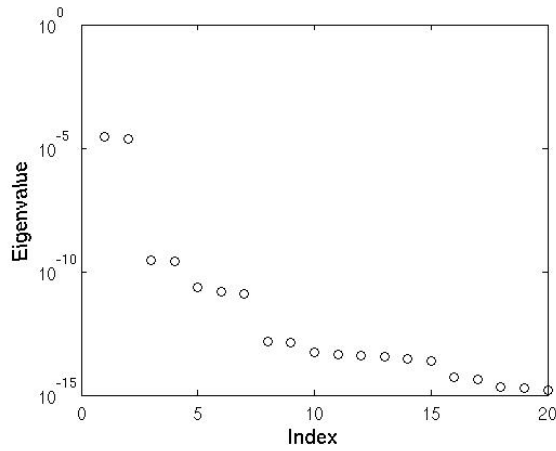



Figure 13: Eigenvalues, square

```

'acousEnFluc'                !-! Variable to post process
10                            !-! Max. number of proper mode to exhibit
'../RUN/SOLUTIONS/mean.h5'    !-! Mean Solution
'../MESH/carre2.coor'         !-! Mesh File
'../MESH/carre2.conn'         !-! Mesh File
'../MESH/carre2.inBound'     !-! Mesh File
'../MESH/carre2.exBound'     !-! Mesh File
'../RUN/SOLUTIONS/carre.sol_0000001.h5' !-! An instantaneous solution
'../RUN/run.dat'              !-! run.dat file
0                             !-! Information no (0) or yes (1)
0                             !-! Scaled spatial (0) or temp. (1) eigenvectors

```

The first step is to consider the eigenvalues, see Fig. 13.

Although the first two eigenvalues are much bigger than the rest, the next two eigenvalues are still bigger than 10^{-10} . So these two will be considered as well.

The next step is to find out if some of the temporal eigenvectors are linked, as they were in section 3. Again the first two temporal eigenvectors are linked, but as well are the third and fourth temporal eigenvector. The parametric representation of the temporal evolution of the last two vectors does not form a circle, but a spiral (see Fig. 14 and 15), which indicates phenomena growing.

The explanation for that is, that the values of the components are not oscillating between two fixed values any more, but they oscillate with growing amplitude. Figure 16 and 17 show the temporal evolution of these four eigenvectors. On the contrary the first two vectors describe a circle underlying the perfect correlation and stability of the phenomena.

As the first and the third temporal eigenvector are significantly different in scale they are normalized to be compared in Fig. 18. It can be seen that these two are closely linked, although the amplitude of the third eigenvector is changing and the scale difference is considerable.

The first two POD modes for u and for p are given in Fig. 19 and 20. They are very similar to the ones in section 3, so no detailed description is given here. They are the “main” solution, the one that is expected (solution of the Helmholtz equation).

The next two modes are “new”. Figure 21 and 22 show these additional modes. The pressure

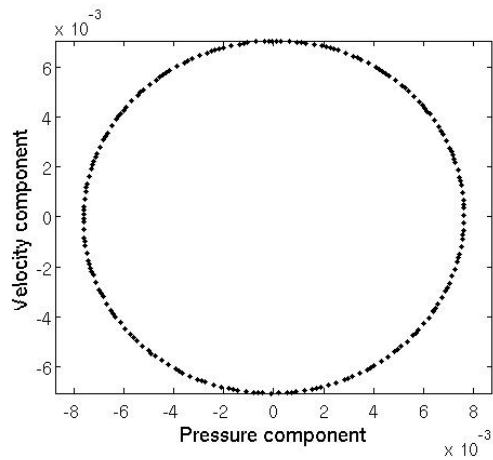


Figure 14: First and second temporal eigenvector, square

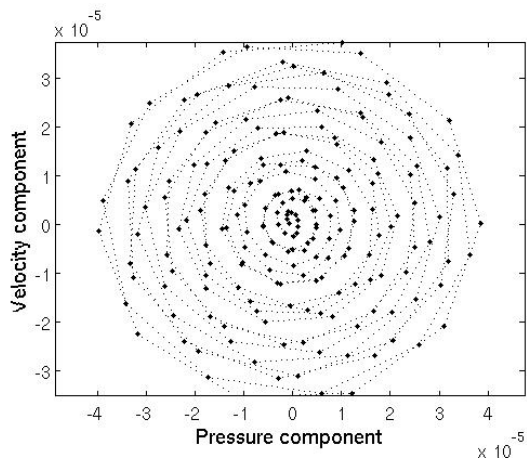


Figure 15: Third and fourth temporal eigenvector, square

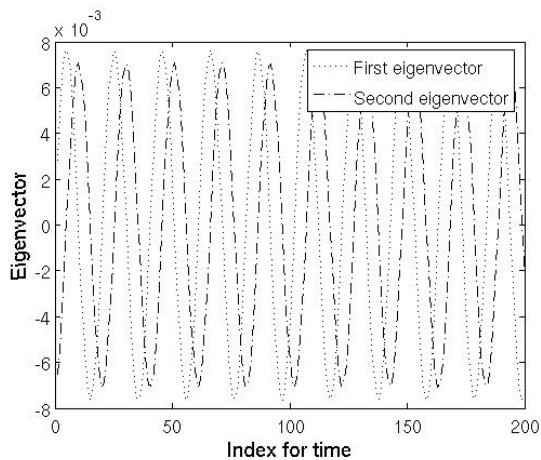


Figure 16: First and second temporal eigenvector evolution, square

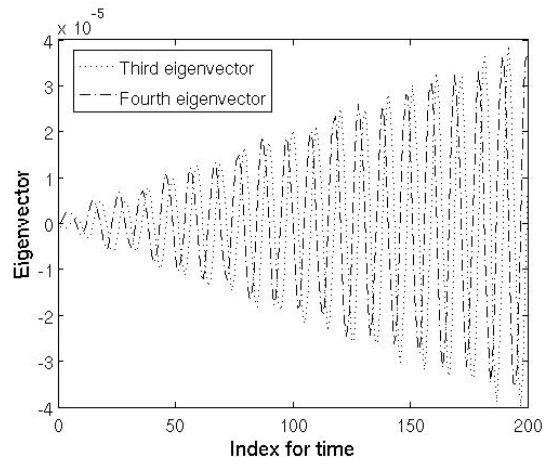


Figure 17: Third and fourth temporal eigenvector evolution, square

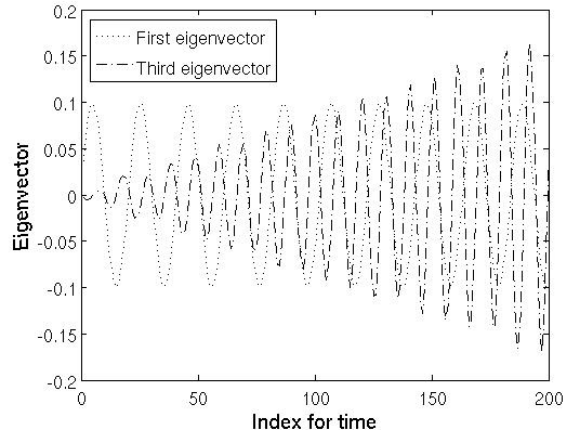


Figure 18: First and third temporal eigenvector evolution, normalized, square

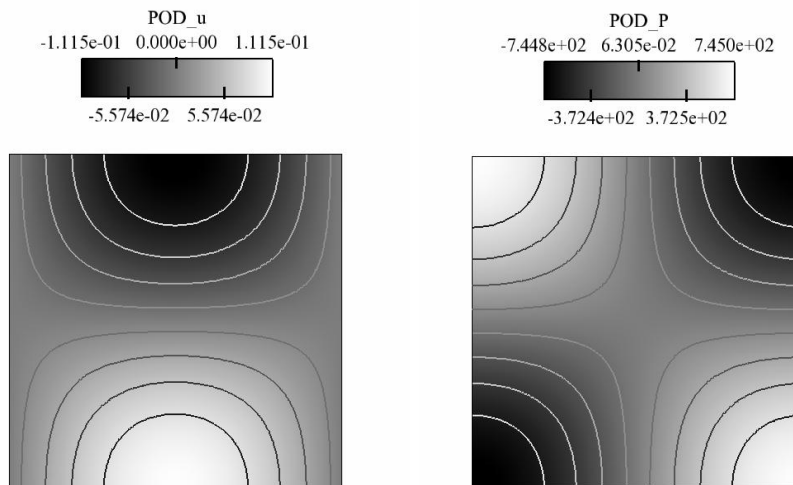


Figure 19: First POD mode, square

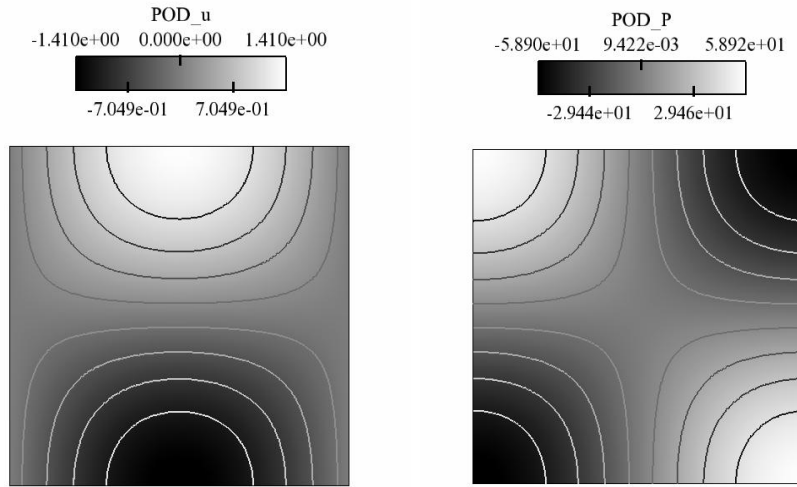


Figure 20: Second POD mode, square

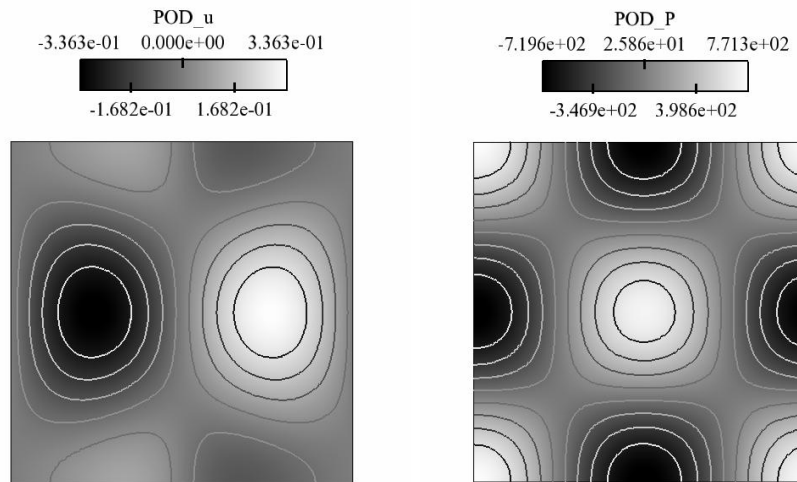


Figure 21: Third POD mode, square

mode of the third POD mode has twice the frequency of the pressure mode of the first two POD modes, and the u component of the fourth POD mode has twice the frequency of the u component of the first two POD modes.

These two modes disturb the “perfect” solution (the first two modes, as it can be seen in the application in section 3) and they are growing in time. It should not be forgotten that the eigenvalues (energies) for these modes are much smaller than the ones for the first two POD modes.

4.3 Conclusions

The first two POD modes are again due to the main solution that was initialized. Although the rest of the POD modes are less important (due to smaller eigenvalues), at least the next two are still structured, as well as their temporal evolution (the temporal eigenvector), and show double frequencies.

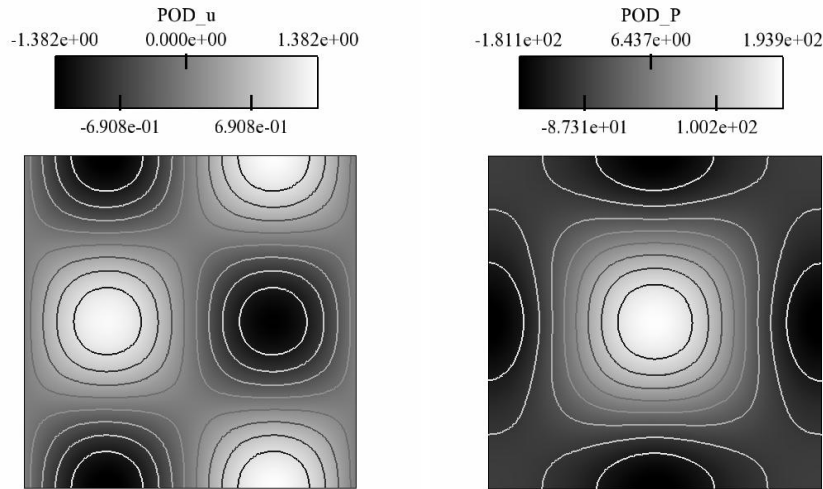


Figure 22: Fourth POD mode, square

5 Application: Square, 3 initial modes

The third application is again on the same domain, but here different modes are initialized to test if the POD algorithm is able to find them.

5.1 AVBP

The snapshot have again been provided by M. Leyko and a short description is given here. The grid used for the AVBP solution is the same as in section 3 (see Fig. 1) and section 4. The initial solution is based on the analytical solution given in Eq. (22)-(24), using $n_x = n_y = 1, 2, 3$, and a shift in between the three different modes to distinguish them. The shift is depending on the frequency of the first mode ($n_x = n_y = 1$) and not a simple factor of it.

run.dat file and asciibound file

The run.dat file used to generate the AVBP solution:

```
'../MESH/carre2'! Mesh file
'./carre.asciiBound' ! AsciiBound file
'dummy' ! AsciiBound_tpf file
'../SOLUTBOUND/carre2.solutBound'! Boundary solution file
'../INIT/init.h5'
'./SOLUTIONS/carre.sol'! output files
'./TIME01/'! temporal evolution directory

1.0d0      ! Reference length | scales coordinates X by X/reflen

1000000    ! Number of iterations

40         ! Number of elements per group (typically of order 100)
1         ! Preprocessor: skip (0), use (1) & write (2) & stop (3)
```

```

1          ! Interactive details of convergence (1) or not (0)
1          ! Prints convergence every x iterations
2          ! Stores solution in separate files (1) or not (0)
5.0d-2     ! final physical time
5.0d-5     ! storage time interval

0          ! Euler (0) or Navier-Stokes (1) calculation
0          ! Additional
0          ! Chemistry
0          ! LES
0          ! TPF
0          ! Artificial viscosity
2          ! Steady state (0) or unsteady (1) calculation
1.0d-5
0 0 0 0 0  ! Scheme specification
3          ! Number of Runge-Kutta stages
0.333333d0 0.5d0 1.0d0      ! Runge-Kutta coefficients
0.7d0      ! CFL parameter for complete update
0.000d0    ! 4th order artificial viscosity coeff.
0.000d0    ! 2nd order artificial viscosity coeff.
0.1d0      ! Fourier parameter for viscous time-step

```

The ascibound file used is:

```

Grid processing by hip version 1.19 'Aardvark'.
4 boundary patches.

```

```

-----
Patch: 1
bottom: y=0
WALL_SLIP_ADIAB

```

```

-----
Patch: 2
right: x=1
WALL_SLIP_ADIAB

```

```

-----
Patch: 3
top: y=1
WALL_SLIP_ADIAB

```

```

-----
Patch: 4
left: x=0
WALL_SLIP_ADIAB

```

5.2 Proper Orthogonal Decomposition

The inner product “PressureFluc” is used for the POD analysis. 1000 snapshots are used and 10 POD modes are calculated.

The avbp2pod.choices file used for the POD analysis is:

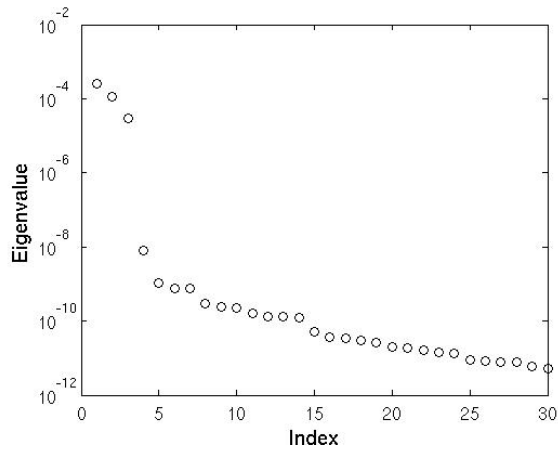


Figure 23: Eigenvalues, square, 3 initial modes

```

'./POD_PressureFluc_scaled_1000/carre.pod'    !-! Output Solution
'../RUN/SOLUTIONS/carre.sol'                 !-! Solution Pattern
0000001                                       !-! Initial Solution
0001000                                       !-! Final Solution
0000001                                       !-! Step
'PressureFluc'                               !-! Variable to post process
10                                           !-! Max. number of proper mode to exhibit
'../RUN/SOLUTIONS/mean.h5'                   !-! Mean Solution
'../MESH/carre2.coor'                         !-! Mesh File
'../MESH/carre2.conn'                         !-! Mesh File
'../MESH/carre2.inBound'                     !-! Mesh File
'../MESH/carre2.exBound'                     !-! Mesh File
'../RUN/SOLUTIONS/carre.sol_0000001.h5'      !-! An instantaneous solution
'../RUN/run.dat'                             !-! run.dat file
1                                             !-! Information no (0) or yes (1)
0                                             !-! Scaled spatial (0) or temp.(1) eigenvector

```

The eigenvalues are shown in Fig. 23 and only the first three temporal and spatial eigenvectors will be considered.

The temporal evolution of the first, the second and the third temporal eigenvalue is shown in Fig. 24 (only the beginning). The first eigenvector has 3 times the frequency, the second twice the frequency of the third eigenvector and they are shifted.

The three different POD modes are shown in Fig. 25 and 26.

The “random” shift between the different modes is important, as problems can occur, if the shift is too perfect (a simple factor of the periode) and the initial modes are too similar. The POD method might not be able to distinguish them properly.

5.3 Conclusions

The POD method was able to find the three different initialized modes for the inner product “PressureFluc”, but the shift between them was important. The different frequencies were found in the temporal eigenvectors as well as in the POD modes.

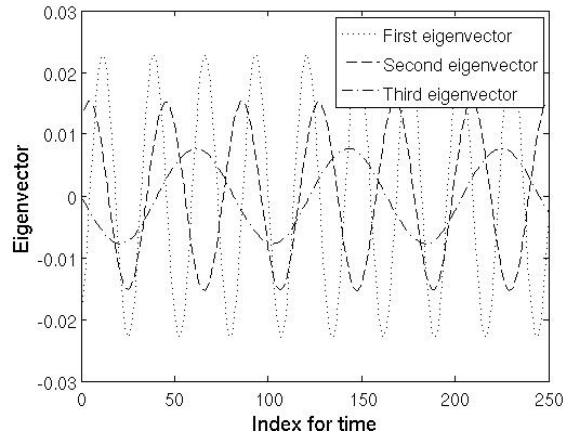


Figure 24: First, second and third temporal eigenvector evolution, square, 3 initial modes

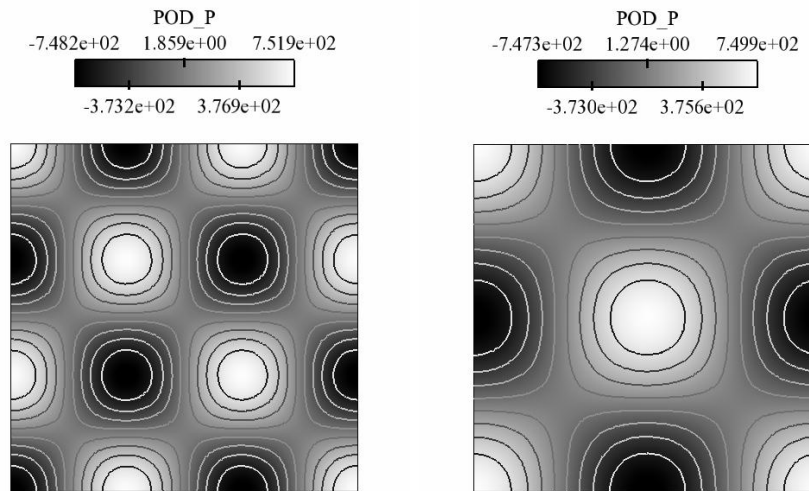


Figure 25: First and second POD mode, square, 3 initial modes

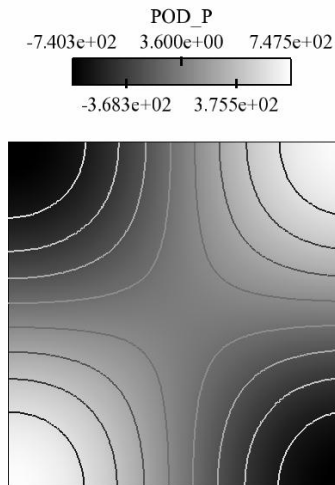


Figure 26: Third POD mode, square, 3 initial modes

6 Application: L-Shape

The fourth application is on a L-shaped domain. A QPF for AVSP is [14], where theoretical considerations can be found, however a short summary of the problem is given here.

The problem for the analytical solution is, that the L-shaped domain conflicts with the separation of the variables, where the boundary conditions should be described independently for the respective variables. The assumption of the separation of variables can be made if the domain is splitted into three squares while additional boundary conditions are used to connect the different squares. The obtained analytical solution is nevertheless incomplete.

6.1 AVBP

The snapshots have again been provided by M. Leyko and correspond to an AVBP run initialized with the same solution for each of three squares as was used in section 4 for the single square (see Eq. (22)-(24)).

The grid used for the AVBP solution is shown in Fig. 27. Every square of the three squares consists of 100×100 grid points.

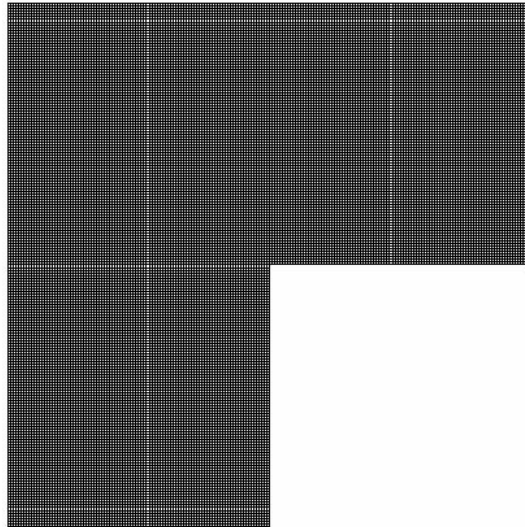


Figure 27: Grid used for AVBP solution, L-Shape

run.dat file and asciibound file

The run.dat file used to generate the snapshots:

```
'../MESH/coin04'! Mesh file
'./coin.asciibound' ! AsciiBound file
'dummy' ! AsciiBound_tpf file
'../SOLUTBOUND/coin04.solutBound'! Boundary solution file
'./SOLUTIONS/coin.sol_0000208.h5'
'./SOLUTIONS/coin.sol'! output files
'./TIME02/'! temporal evolution directory
```

```

1.0d0      ! Reference length | scales coordinates X by X/reflen

1000000    ! Number of iterations

40         ! Number of elements per group (typically of order 100)
1         ! Preprocessor: skip (0), use (1) & write (2) & stop (3)

1         ! Interactive details of convergence (1) or not (0)
1         ! Prints convergence every x iterations
2         ! Stores solution in separate files (1) or not (0)
10.0d-2    ! final physical time
20.0d-5    ! storage time interval

0         ! Euler (0) or Navier-Stokes (1) calculation
0         ! Additional
0         ! Chemistry
0         ! LES
0         ! TPF
0         ! Artificial viscosity
1         ! Steady state (0) or unsteady (1) calculation

0 0 0 0 0  ! Scheme specification
3         ! Number of Runge-Kutta stages
0.333333d0 0.5d0 1.0d0      ! Runge-Kutta coefficients
0.7d0      ! CFL parameter for complete update
0.000d0    ! 4th order artificial viscosity coeff.
0.000d0    ! 2nd order artificial viscosity coeff.
0.1d0      ! Fourier parameter for viscous time-step

```

the asciibound file:

```

Grid processing by hip version 1.19 'Aardvark'.
3 boundary patches.

```

```

-----
Patch: 1
Wall
WALL_SLIP_ADIAB

```

```

-----
Patch: 2
sym1
SYMMETRY

```

```

-----
Patch: 3
sym2
SYMMETRY

```

6.2 Proper Orthogonal Decomposition

The same inner product is applied as in the applications before (“acousEnFluc”, see Eq. (27)), 200 snapshots are used and 10 POD modes are calculated.

The eigenvalues are shown in Fig. 28.

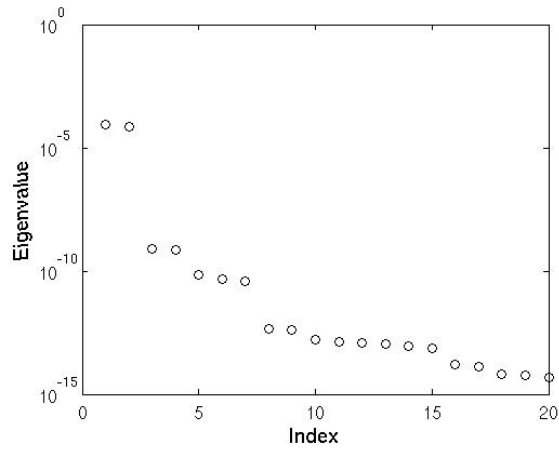


Figure 28: Eigenvalues, L-Shape

The same links between the different temporal eigenvectors occur as in section 4. That is not surprising, as the L-shaped domain was divided into three squares and the same kind of initial solution as in section 4 was used on every square.

The temporal evolution of the first two eigenvectors is shown in Fig. 29, the third and fourth eigenvector are shown in Fig. 30. Again the same structure can be observed as in section 4.

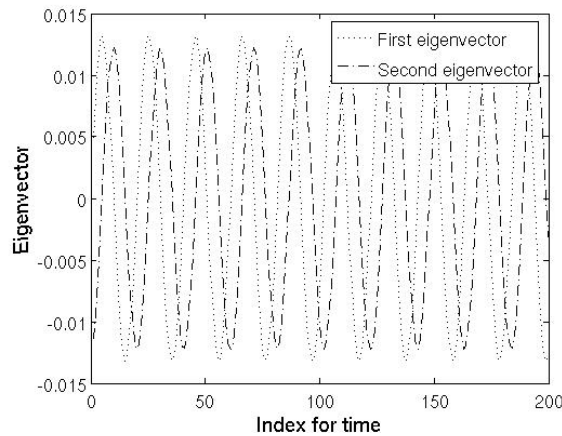


Figure 29: First and second temporal eigenvector evolution, L-Shape

To find the connection between the first and the third eigenvector, which are both linked to the pressure, they have to be normalized again. Figure 31 shows these two eigenvectors.

The POD modes for this applications can be seen in Fig. 32-35, and again the similarity to the POD modes of section 4 are obvious. So the same explanations can be used for the L-shaped domain.

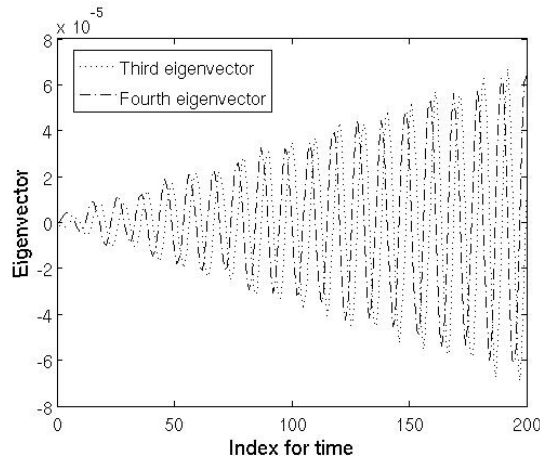


Figure 30: Third and fourth temporal eigenvector evolution, L-Shape

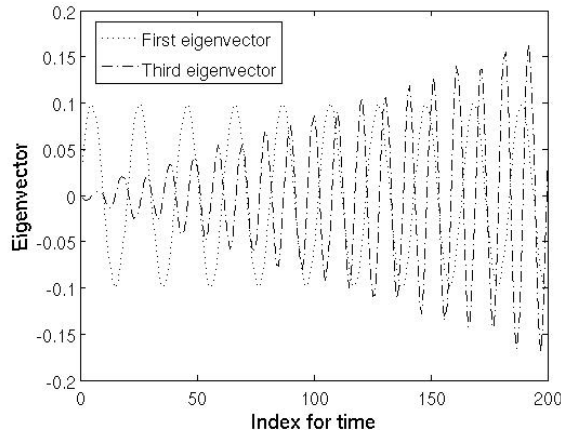


Figure 31: First and third temporal eigenvector evolution, normalized, L-Shape

6.3 Conclusions

Although this L-shaped domain seems to be quite different from the two applications of section 3 and 4, the fact that the initial solution on the subdomains is the same as in the sections before (except section 5) as well as the grids on the subdomains, leads to quite similar results.

7 Conclusions

The POD method has been used for four different applications, that had strong links between each other. Different inner product have been used.

The POD was able to find the initialized modes in all applications, but in some cases other modes were found as well. These modes were much less important than the initialized modes, due to the smaller eigenvalues, but they were still structured. In the application with more than one initialized mode the time shift in between them was important to distinguish the different modes.

In all cases “double” modes occurred while using the key variable “acousEnFluc” because of time shift of the fluctuation in pressure and in velocity.

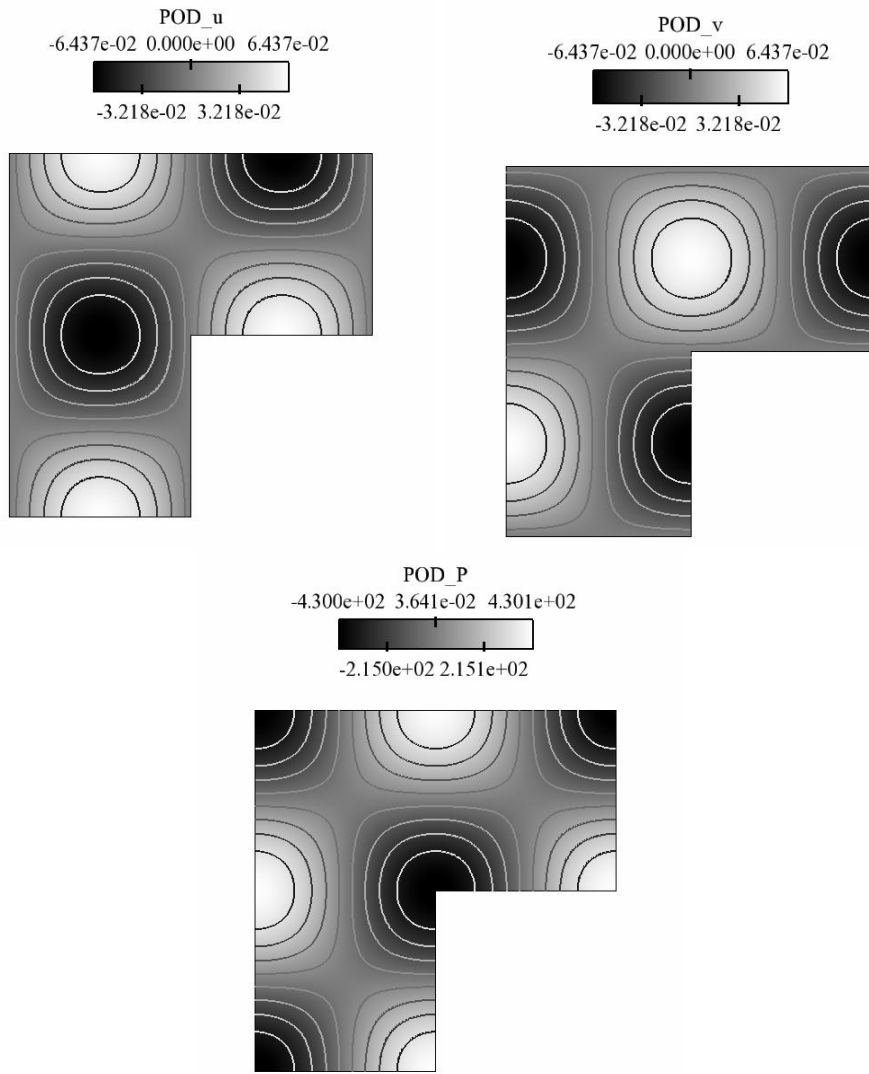


Figure 32: First POD mode, L-Shape

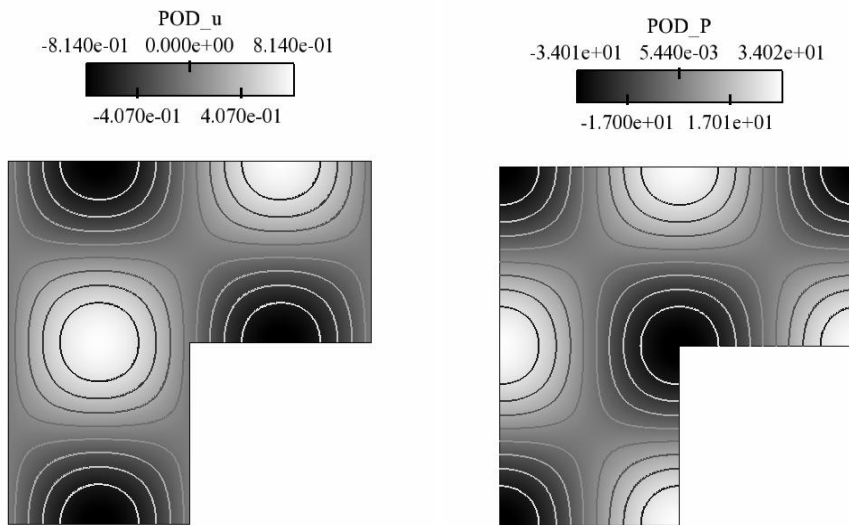


Figure 33: Second POD mode, L-Shape

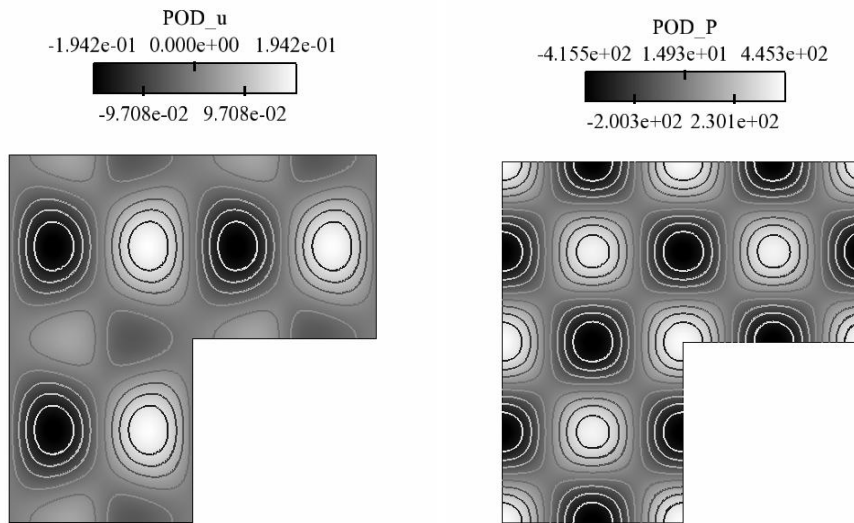


Figure 34: Third POD mode, L-Shape

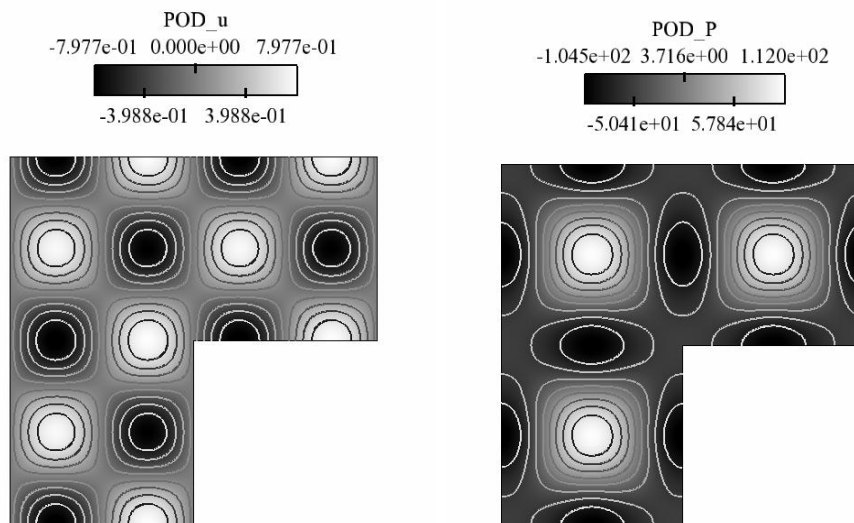


Figure 35: Fourth POD mode, L-Shape

Annex - How to use POD

This annex gives a short description of how to use POD to analyse an AVBP solution.

Input files

In the POD-directory there have to be the `avbp2pod.choices` file, that will be explained later, the `input_*.dat` files of the AVBP run and the batch file for submission. There should also be a directory in which the POD modes will be stored.

Further the snapshots that should be analyzed, the `run.dat` file, the mesh files `.coor`, `.conn`, `.inBound`, `.exBound`, as well as a mean solution are needed.

avbp2pod.choices file

A short explanation of how to fill in the `avbp2pod.choices` file is given here.

```
(1) './POD_acousEnFluc_scaled/carre.pod'    !-! Output Solution
(2) './RUN/SOLUTIONS/carre.sol'           !-! Solution Pattern
(3) 0000001                               !-! Initial Solution
(4) 0000200                               !-! Final Solution
(5) 0000001                               !-! Step
(6) 'acousEnFluc'                         !-! Variable to post process
(7) 10                                     !-! Max. number of proper mode to exhibit
(8) './RUN/SOLUTIONS/mean.h5'             !-! Mean Solution
(9) './MESH/carre2.coor'                  !-! Mesh File
(10) './MESH/carre2.conn'                 !-! Mesh File
(11) './MESH/carre2.inBound'              !-! Mesh File
(12) './MESH/carre2.exBound'              !-! Mesh File
(13) './RUN/SOLUTIONS/carre.sol_0000001.h5' !-! An instantaneous solution
(14) './RUN/run.dat'                      !-! run.dat file
(15) 0                                     !-! Information no (0) or yes (1)
(16) 0                                     !-! Scaled spatial (0) or temp. (1) eigenvectors
```

- In line (1) the name and the directory of the POD modes that are calculated by the algorithm have to be chosen.
- With line (2)-(5) the AVBP solutions that should be used for performing POD are selected. So the directory and the name as well as the the first, the last solution and the step in between have to be specified. For this example the 200 files “`carre.sol_0000001.h5`” to “`carre.sol_0000200.h5`” in the directory “`./RUN/SOLUTIONS/`” are used.
- Line (6) selects the key variable that chooses the inner product used for the POD analysis, for example
 - pressure, `PressureFluc`
 - velocity, `primevelocity`, `u`, `v`
 - acousticEnergy, `acousEnFluc`

For more information about the different inner product see section 2, Eq. (8)-(10).

- In line (7) the maximum number of POD modes that should be calculated is chosen. This can be a difficult a priori choice as the corresponding eigenvalues are useful hint of the importance of a mode. But they are not known before running the POD algorithm.
- The lines (8)-(14) have to be filled in with the information of the AVBP run.
- With line (15) additional information about the the temporal eigenvectors and -values can be obtained. The correlation matrix is a real symmetric matrix and should have real eigenvalues. Due to the numerical solving of the eigenvalue problem complex eigenvectors and -values can occur. For example if the key variable “pressure” is used, the mean value is very big compared to the fluctuation. So the entries of the correlation matrix are quite similar compared to their absolut size, which can cause difficulties in solving the eigenvalue problem. Not all eigenvalues and -vectors are used in the POD algorithm (see line (7)), so there is only a warning if the ones used have an imaginay part. This imaginay part is skipped and the real part is put in the computation. If there is a (1) in this line information about these problems of all eigenvectors and -values is displayed, not only for those that are actually used.
- Line (16) is for chosing the scaling. The method described in this report is for controlled scaling of the spatial eigenvectors (that is usually found in the theory for POD). To apply this method use “0” in this line. This leads to temporal eigenvectors, that differ significantly in scale. It can be used to compare the importance of the POD modes. For this case it is necessary to divide by the eigenvalues in the POD algorithm, that can be very small. If they are smaller than 10^{-15} this division is not performed any more with a warning. To avoid this less POD modes can be calculated. These modes without proper scaling should not be used.

Another way to avoid this problem is not to control the scaling of the spatial but the temporal eigenvector (use “1” in this line). This leads to similar temporal eigenvectors in size and the information of the importance is contained in the POD modes, that will differ in scale. An advantage is that the division by the eigenvalue is not necessary in this case.

Output files

The output files of POD are

- `pod_matrix.dat` (the correlation matrix),
- `pod_val_p.dat` (the eigenvalues),
- `pod_vect_p.dat` (the temporal eigenvectors),
- POD modes in the selected directory with the selected name (for example `./POD_acousEnFluc_scaled/carre.pod_0000001.h5`),
- it is recommended to redirect the standard output to a file where warnings and information are displayed.

The POD modes are given in an AVBP mean format so they can be visualized using a visual script.

List of Figures

1	Grid used for AVBP solution, “perfect” square	6
2	Eigenvalues, “perfect” square, pressure fluctuation	7
3	First temporal eigenvector evolution, “perfect” square, pressure fluctuation	7
4	First POD mode, “perfect” square, pressure fluctuation	8
5	Eigenvalues, “perfect” square, velocity fluctuation	8
6	First temporal eigenvector evolution, “perfect” square, pressure and velocity fluctuation	9
7	First POD mode, “perfect” square, velocity fluctuation	9
8	Eigenvalues, “perfect” square, acoustic energy fluctuation	10
9	First and second temporal eigenvector, “perfect” square, acoustic energy fluctuation	11
10	First and second temporal eigenvector evolution, “perfect” square, acoustic energy fluctuation	11
11	First POD mode, “perfect” square, acoustic energy fluctuation	12
12	Second POD mode, “perfect” square, acoustic energy fluctuation	12
13	Eigenvalues, square	15
14	First and second temporal eigenvector, square	16
15	Third and fourth temporal eigenvector, square	16
16	First and second temporal eigenvector evolution, square	16
17	Third and fourth temporal eigenvector evolution, square	17
18	First and third temporal eigenvector evolution, normalized, square	17
19	First POD mode, square	17
20	Second POD mode, square	18
21	Third POD mode, square	18
22	Fourth POD mode, square	19
23	Eigenvalues, square, 3 initial modes	21
24	First, second and third temporal eigenvector evolution, square, 3 initial modes	22
25	First and second POD mode, square, 3 initial modes	22
26	Third POD mode, square, 3 initial modes	22
27	Grid used for AVBP solution, L-Shape	23
28	Eigenvalues, L-Shape	25
29	First and second temporal eigenvector evolution, L-Shape	25

30	Third and fourth temporal eigenvector evolution, L-Shape	26
31	First and third temporal eigenvector evolution, normalized, L-Shape	26
32	First POD mode, L-Shape	27
33	Second POD mode, L-Shape	27
34	Third POD mode, L-Shape	28
35	Fourth POD mode, L-Shape	28

References

- [1] BERKOOZ, G., HOLMES, P., AND LUMLEY, J. The Proper Orthogonal Decomposition in the Analysis of Turbulent Flows. *Annual Review of Fluid Mechanics* 25 (1993), 539–575.
- [2] BRAUD, C. *Étude de la dynamique d'un écoulement à cisaillements croisés: interaction couche de mélange-sillage*. PhD thesis, Poitiers University, France, 2003.
- [3] CHATTERJEE, A. An introduction to the proper orthogonal decomposition. *Current Science* 78, 7 (2000), 808–817.
- [4] CORDIER, L., AND BERGMANN, M. Proper Orthogonal Decomposition: an Overview. *Post Processing of Experimental and Numerical Data* (2003), 1–45. Lecture Series 2003/2004, von Karman Institut for Fluid Dynamics.
- [5] HOLMES, P., LUMLEY, J., AND BERKOOZ, G. Turbulence, Coherent Structures, Dynamical Systems and Symmetry. *Cambridge Monographs on Mechanics*. Cambridge University Press (1996).
- [6] HUANG, Y., WANG, S., AND YANG, V. Systematic Analysis of Lean-Premixed Swirl-Stabilized Combustion. *AIAA Journal* 44, 4 (2006), 724–740.
- [7] LUMLEY, J. The structure of inhomogeneous turbulent flows. *Atmospheric Turbulence and Radio Wave Propagation* (1967), 166–178. ed. A. Yaglom and V. Tatarski.
- [8] POINSOT, T., AND VEYNANTE, D. *Theoretical and Numerical Combustion*. Edwards, 2001.
- [9] ROUX, A., GICQUEL, L., SOMMERER, Y., AND POINSOT, T. Large eddy simulation of mean and oscillating flow in side-dump ramjet combustor. *Combust. Flame in press* (2007).
- [10] ROUX, S. Application de la décomposition en modes propres à des calculs de simulations aux grandes échelles. Rapport de stage 2ème année Ingénieur - ENSEEIHT WN/CFD/06/61, CERFACS, September 28 2006.
- [11] ROWLEY, C., COLONIUS, T., AND MURRAY, R. Model Reduction for Compressible Flows Using POD and Galerkin Projection. *Physica. D* 189 (2004), 115–129.
- [12] SILVA, C. AVSP Quality Program Form, Square cavity. Tech. rep., CERFACS, Internal Document, 2007. AVSP V4.0.
- [13] SIROVICH, L. Turbulence and the Dynamics of Coherent Structures. Part 1: Coherent Structures. *Quarterly of Applied Mathematics* 45, 3 (1987), 561–571.

- [14] WIECZOREK, K. AVSP Quality Program Form, L-Shape. Tech. rep., CERFACS, Internal Document, 2007. AVSP V4.0.